NANO LETTERS

Letter

pubs.acs.org/NanoLett

Surface-Enhanced Raman Scattering with Ag Nanoparticles Optically Trapped by a Photonic Crystal Cavity

Shiyun Lin, Wenqi Zhu, Yuhang Jin, and Kenneth B. Crozier*

School of Engineering and Applied Sciences, Harvard University, 33 Oxford Street, Cambridge, Massachusetts 02138, United States

Supporting Information

ABSTRACT: We demonstrate a reusable and reconfigurable surface enhanced Raman scattering (SERS) platform by optically trapping Ag nanoparticles with a photonic crystal cavity integrated with a microfluidic chip. High-performance SERS is performed in a very reproducible manner, owing to the fact that Ag aggregates are produced by optical trapping in a controllable process that is monitored in real-time by the cavity resonance shift that occurs with the trapping of each additional nanoparticle.

KEYWORDS: *Optical trapping, SERS, silicon photonics, resonator*

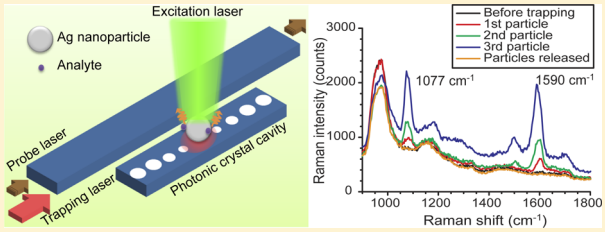

Surface enhanced Raman scattering (SERS) enables molecules to be identified by their vibrational "fingerprints".[1−3] SERS applications range from the detection of biological warfare agents such as anthrax,[4] to explosives,[5] to pollutants such as arsenic in drinking water,[6] to contaminants in foods (e.g., melamine in milk),[7] to glucose levels measured in vivo.[8] To overcome the fact that Raman cross sections are small, a variety of SERS substrates with large field enhancements have been developed, including nanoparticle colloids,[9−13] rough metallic surfaces,[14] and nanoantennas.[15−19] SERS substrates based on colloidal metal nanoparticles and rough metallic surfaces are inexpensive and easy to prepare but rely on processes over which there is little or no control. Plasmonic structures produced by top-down nanofabrication possess high signal enhancement and controllability but require complex fabrication processes. In almost all cases, these substrates are only one-time-use because the molecules bind very strongly to them. That SERS substrates generally need to be discarded after use has two principal disadvantages. The first is that of cost. The second is that it renders them unsuitable for applications for which manual human intervention to replace the SERS substrate is infeasible, for example, unattended systems for the continual monitoring of chemicals in air and water. A high-performance substrate that could be refreshed at-will would be a new paradigm in SERS sensing. Here, we demonstrate such a device by trapping Ag nanoparticles using an on-chip optical cavity.[20−23] The Raman emission from molecules on the surfaces of the nanoparticles is enhanced due to the large electromagnetic fields there. We demonstrate that the resonance shift of the cavity enables monitoring of trapped nanoparticles, which make the controllable assembly of Ag aggregations possible. We note that this functionality was not present in recent optical trapping-assisted SERS experiments with traditional optical tweezers[24,25] and light-induced optoelectrofluidics.[26] We demonstrate that turning the laser off then on again results in the nanoparticles being released and fresh particles being trapped. Our device has not only the advantage of reusability but also that of reconfigurability. Nanoparticles of different sizes, shapes, materials and surface functionalizations could be supplied to the chip. The type of nanoparticles to be trapped could be chosen based on the chemical to be sensed.

Figure 1a shows a schematic diagram of the trapping-assisted SERS platform we introduce. Analyte molecules (4-aminothiophenol (pMA) or 2-naphthalenethiol (2-NT) purchased from Sigma-Aldrich Co. LLC) are first mixed with Ag nanoparticles with diameters of 80 nm. The Ag nanoparticles are purchased from BBinternational and are stabilized by citrate. The mixed samples are left for 24−48 h at room temperature before the measurements. The nanoparticles onto which the analyte molecules have bound are then sent into a microfluidic channel and optically trapped by a photonic crystal cavity that is situated at the bottom of the channel. The beam from a trapping laser is combined with that from a second (lower-power) probe laser and input to the device. Both the trapping and probe lasers have operating wavelengths around 1550 nm. The probe laser is continually swept in wavelength, enabling the resonance wavelength of the optical cavity to be monitored. An upright homemade microscope is used to measure Raman scattering from molecules on the optically trapped nanoparticles with excitation from a green laser (λ = 532 nm). Further details on the trapping platform are included in Supporting Information S1.

We choose to use a photonic crystal cavity because its small mode volume and large field enhancement[21] enable a large optical force enhancement for trapping Ag nanoparticles. The silicon photonic crystal cavities and waveguides are fabricated

Received: November 4, 2012
Revised: January 8, 2013

   dx.doi.org/10.1021/nl304069n | *Nano Lett.* XXXX, XXX, XXX−XXX

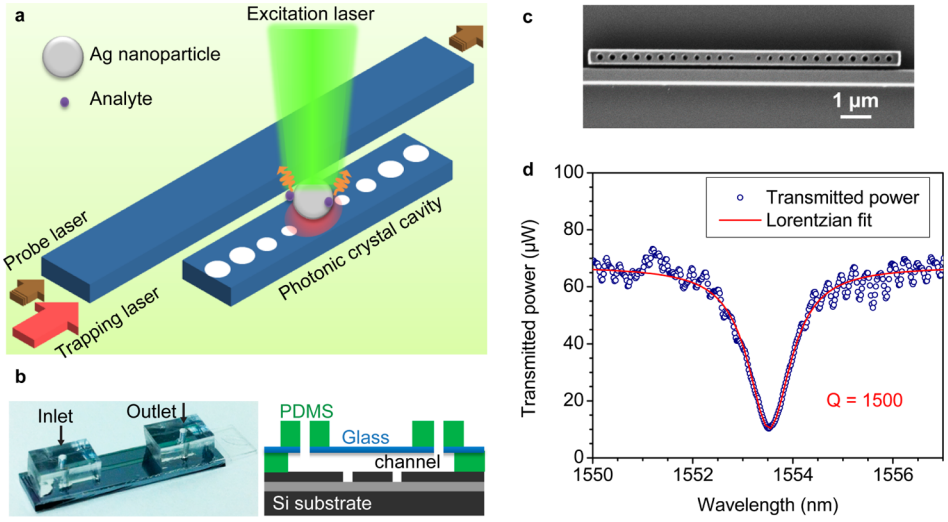

Figure 1. Trapping-assisted SERS platform. (a) Schematic diagram of trapping-assisted SERS platform. (b) Left: photograph of fabricated device that integrates microfluidic channel with silicon photonic chip. Right: schematic diagram of device cross section. (c) SEM image of silicon photonic crystal cavity coupled to waveguide with a gap of 200 nm. (d) Measured transmission spectrum and Lorentzian curve fit, showing a Q of 1500.

on a SOI wafer with a 220 nm thick Si layer and 3 μm thick buried oxide.[27] The wafer is first cleaved and coated with negative tone e-beam resist (hydrogen silsesquioxane, HSQ), followed by electron beam lithography and reactive ion etching. Smooth and vertical sidewalls are achieved via the use of hydrogen bromide (HBr) gas as the Si etchant. The remaining HSQ is removed by dipping the chip into 7:1 buffered oxide etch (BOE) solution. A thin PDMS film (100 μm thick) with a 1 mm wide channel cut in the center is bonded to the silicon chip. A glass coverslip (no. 1.5) is then bonded to the top of the PDMS. The coverslip contains two holes that are drilled into it by a high power CO_2 laser. Two thick PDMS chunks are then bonded to the coverslip to enable inlet and outlet tubes to be attached to the device. Figure 1b shows a photograph of the final device. Figure 1c shows a scanning electron microscope top-view image of the fabricated photonic crystal cavity coupled to a waveguide. The waveguides are 450 nm wide and 220 nm thick. The holes are shifted outward to form a cavity in the center. Tapered sections with hole diameters that gradually increase from the cavity center are incorporated to reduce the scattering loss of the cavity mode and to improve the quality factor. Figure 1d shows the measured transmission spectrum of the cavity. The Lorentzian fit shows a quality factor (Q) of 1500.

We first demonstrate the trapping of 80 nm Ag nanoparticles on the bus waveguide and the photonic crystal cavity. The trapping laser is set so that both a transverse electric (TE) mode (50% power) and a transverse magnetic (TM) mode (50% power) are excited. The TM mode traps nanoparticles on the waveguide more effectively than the TE mode since it has a stronger evanescent field and thus exerts a larger optical force. The wavelength is set to the resonance wavelength of the photonic crystal cavity, meaning that the TE mode can couple to it. The field enhancement, a consequence of the high Q factor and small mode volume of the cavity, enables nanoparticles to be readily trapped on it. The Supporting Information video shows an Ag nanoparticle that is trapped on the waveguide by the gradient force and propelled along it by the scattering force. When it reaches the photonic crystal cavity, it is pulled onto it and trapped.

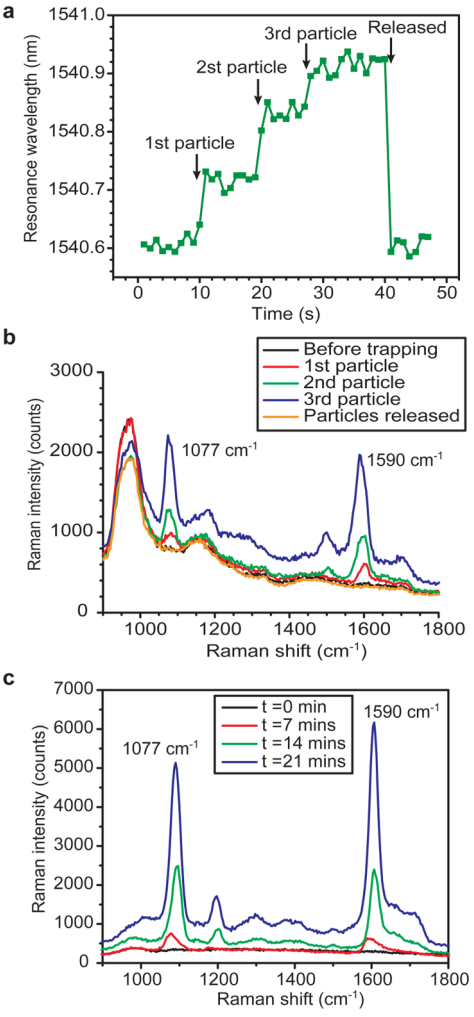

Figure 2. SERS hotspots generated by trapping Ag nanoparticles in a controllable manner. (a) Resonance wavelength shift as particles are trapped, as measured by probe laser. (b) SERS spectra measured with different numbers of particles trapped. (c) SERS spectra measured with Ag nanoparticle aggregations of different sizes formed at different times.

dx.doi.org/10.1021/nl304069n | *Nano Lett.* XXXX, XXX, XXX−XXX

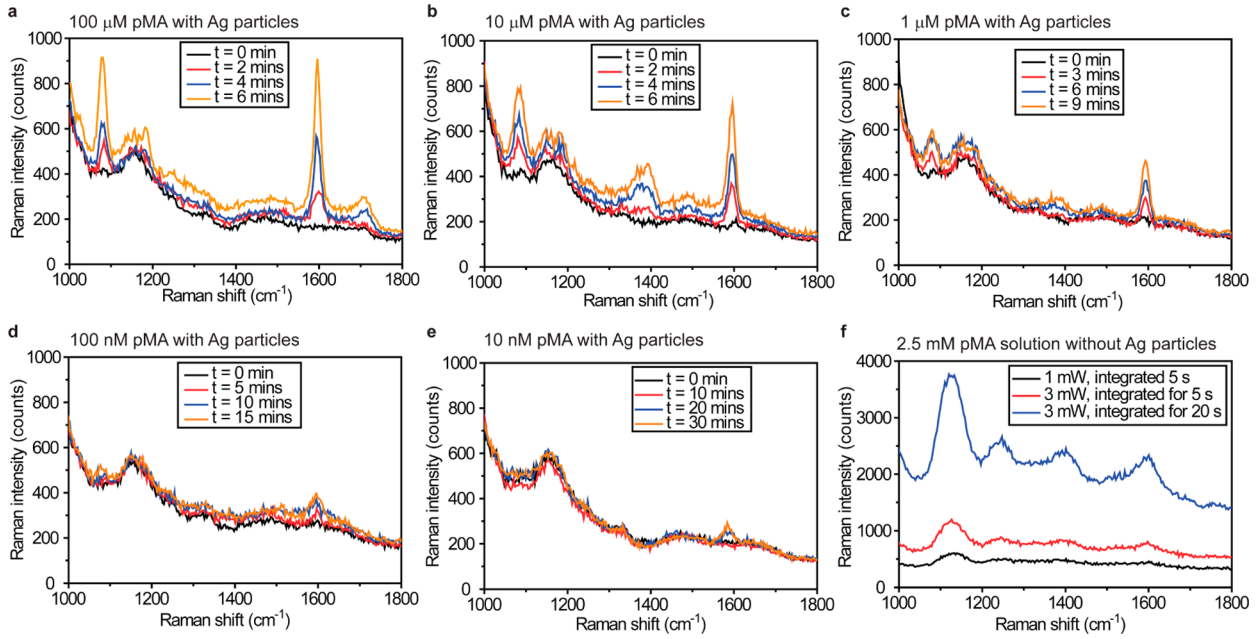

Figure 3. SERS performance for low concentration samples. (a–e) Raman spectra measured by the trapping-assisted approach for samples with different pMA concentrations: (a) 100 μM, (b) 10 μM, (c) 1 μM, (d) 100 nM, and (e) 10 nM. Laser power for SERS excitation is 1 mW, and spectrometer integration time is 5 s for all measurements in (a–e). (f) Raman spectra measured for reference sample without Ag nanoparticles.

In addition to trapping nanoparticles, the waveguide-coupled cavity enables the monitoring of the trapped nanoparticles by measuring the cavity resonance shift using the probe laser.[28] Figure 2a shows the resonance shift as a function of time after the trapping laser is turned on. The probe laser is continually swept in wavelength at 5 nm/s over a range of 5 nm. The resonance wavelength is found from each scan by fitting the transmission spectrum with a Lorentzian function. The trapping laser is turned on at t = 0 s. It can be seen that resonance wavelength jumps of ~0.1 nm occur with each additional nanoparticle being trapped. After turning off the trapping laser at ~40 s, the resonance wavelength returns to its value before the first particle was trapped. That the particles can be released by turning off the trapping laser confirms that the trapping process is indeed optical in nature. SERS spectra measured during the trapping process, recorded at each resonance wavelength step (Figure 2a), are shown in Figure 2b. The solution contains pMA (250 μM concentration), Ag nanoparticles (1.72 pM), deionized water, and acetone. The laser power for SERS excitation is 3 mW and the spectrometer integration time is 10 s. The Raman spectrum after releasing trapped nanoparticles is also shown. Within the measured Raman shift range (900–1800 cm^{-1}), there are two peaks originating from the pMA molecules (1077 and 1590 cm^{-1}).[29] No pMA Raman peaks are observed before trapping the nanoparticles. The Raman counts at the wavenumbers corresponding to the pMA peaks increase with the number of trapped particles. The SERS enhancement factors (EFs) are calculated to be 2.3 × 10^3, 2.8 × 10^3, and 4.1 × 10^3, for the one-, two-, and three-particle cases, respectively. These represent the average values by which Raman scattering for all molecules on the nanoparticle surfaces are increased, compared to the reference case of the molecules being in pMA solution (without the nanoparticles). It should be stressed that these are average values; the EF for molecules in the hotspot regions is inevitably much higher. The method by which the EFs are calculated is described in detail in Supporting Information S2 and S3. After turning off the trapping laser, the Raman spectrum also returns to its original state before the first particle was trapped, as shown in the orange curve of Figure 2b. This demonstrates that our approach enables a surface-enhanced hotspot (i.e., the optically trapped nanoparticles) to be formed and released in a controllable manner.

In Figure 2c, we demonstrate that the SERS signal can be enhanced further by keeping the trapping laser on to form larger nanoparticle clusters. The laser power used for SERS excitation is 1 mW and spectrometer integration time is 5 s. SERS spectra are measured at different times after turning on the trapping laser. At 21 min, the measured signal, divided by the laser power and spectrometer integration time, is 140 times larger than that of the single particle case in Figure 2b. The drawback of trapping these large clusters is that they become irreversibly stuck to the cavity surface much more readily due to the large gradient force and long trapping time.

The demonstrated high SERS enhancement could be advantageous in applications that require sensing analytes at low concentrations. To quantify the performance of our controllable platform, the SERS spectra of pMA solutions with concentrations ranging from 100 μM to 10 nM are measured (Figure 3a–e). The pMA solutions are first mixed with Ag nanoparticles at room temperature and left for 48 h before measurement. Similar to Figure 2c, the Raman intensity increases with trapping time due to the formation of large Ag nanoparticle aggregations. The Raman intensities for the pMA samples with lower concentrations are smaller, even with the larger Ag aggregations that result from the longer trapping times employed. In the higher concentration samples, the pMA molecules cover a large fraction of the surface area of the trapped Ag nanoparticles, leading to a larger Raman signal. We successfully detect pMA molecules with concentrations down to 10 nM. We also measure a reference sample with 2.5 mM pMA molecules that does not contain any Ag nanoparticles

dx.doi.org/10.1021/nl304069n | Nano Lett. XXXX, XXX, XXX–XXX

(Figure 3f). A large excitation power (3 mW) and long integration time (20 s) are used in order to obtain an observable Raman signal. Using these results, we calculate the analytical enhancement factor (AEF) using[30]

$$\mathrm{AEF} = \frac{\frac{I_{\mathrm{SERS}}}{c_{\mathrm{SERS}}}}{\frac{I_{\mathrm{R}}}{c_{\mathrm{R}}}} \quad (1)$$

where I_{SERS} and C_{SERS} are the measured Raman intensity and concentration, respectively, for the SERS sample. Similarly, I_{R} and C_{R} are the intensity and concentration, respectively, for the reference sample. Using the data for the 10 nM and reference samples (Figure 3e,f), the AEF is found to be 5×10^5, a value comparable to that achieved by SERS substrates consisting of aggregates of colloidal Ag nanoparticles.[13,30]

The ability of our approach to generate SERS hotspots on demand in a highly controllable manner presents the exciting opportunity for the detection of multiple analytes. To demonstrate this, we perform an experiment where we inject pMA and 2-NT solutions to the chip in an alternating fashion. Figure 4 shows that when each type of analyte is injected, only its corresponding SERS peaks are observed. Both pMA and 2-NT molecules are mixed with Ag nanoparticles and incubated for 24 h before measurement. The results confirm the ability of the device to produce a SERS hotspot that can be continually replenished by trapping new nanoparticles. Indeed, we confirm that by keeping the trapping power low enough to prevent nanoparticles from sticking to the surface irreversibly the device can be used for days.

In our approach, the field distributions produced by a photonic crystal cavity generates an optical trapping potential. For a given number of nanoparticles, there will be a configuration that minimizes the potential energy. The nanoparticles will ideally be trapped into this configuration. The presence of Brownian motion and fluctuations due to other factors, such as unintentional fluid flow due to instabilities in the microfluidic channel, in practice means that there is some uncertainty in the precise configuration into which the nanoparticles are trapped. Our method, nonetheless, presents an opportunity for nanoparticle clusters for SERS to be formed in a highly reproducible manner since their formation is guided by optical forces, rather than occurring in a random fashion via salt-induced aggregation. We furthermore note that the cluster formation is monitored in real-time. We anticipate that the engineering of photonic crystal cavities to produce trapping potentials that trap nanoparticles into predefined favorable configurations in a very precise manner would be an exciting direction for future research.

In conclusion, we demonstrate a controllable and reusable SERS platform using Ag nanoparticles optically trapped by an on-chip photonic crystal cavity. The nanoparticle aggregations are assembled in a highly reproducible fashion that is monitored by measuring the resonance shift of the cavity. The nanoparticles can be released after a SERS measurement is made by turning off the trapping laser. We demonstrate SERS performance (analytical enhancement factor) that is on par with current approaches based on the salt-induced aggregation of Ag colloids but that has the advantage of the aggregates being assembled controllably. We anticipate that this work could open a new paradigm for reusable SERS sensors, particularly for the sensing of multiple species in applications for which intervention to replace the SERS substrate is impractical. More generally, however, it presents a means for assembling nanomaterials produced in solution (e.g., quantum dots or plasmon nanoparticles) on a chip in a highly controllable manner.

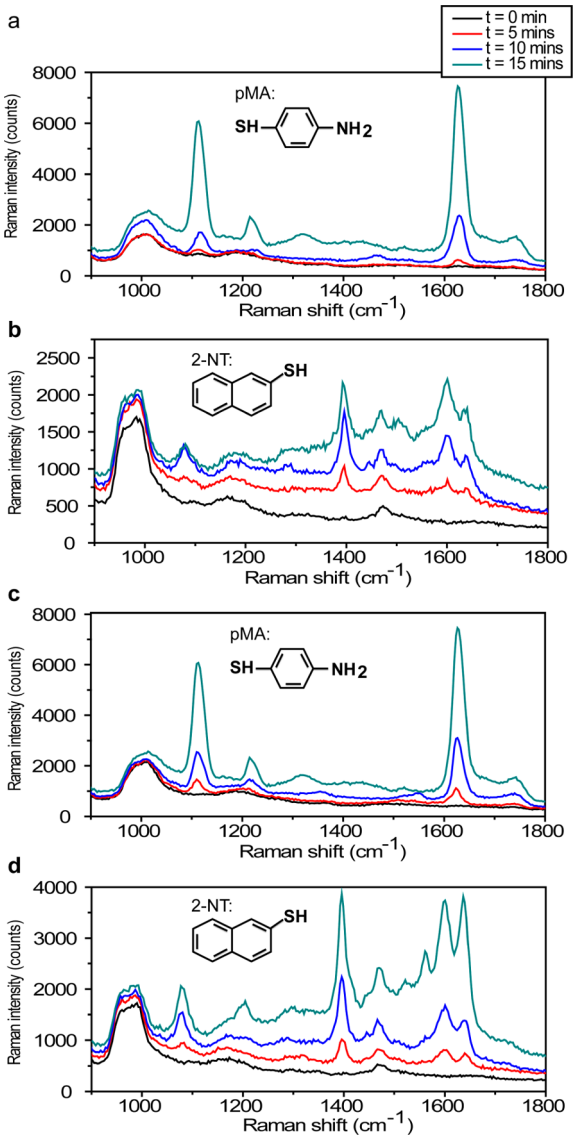

Figure 4. Exchanging analyte. (a–d), Raman spectra measured when alternately injecting pMA and 2-NT samples into the chip. Insets show chemical structure of corresponding molecule. SERS spectra are measured after turning on trapping laser for 0, 5, 10, and 15 min. (a). Chip is cleaned by flushing by DI water to remove the previous analyte. Following cleaning, 2-NT is injected and SERS measurements are performed under same conditions (b). Similarly, (c) and (d) show results for second round of injecting pMA and 2-NT samples, respectively. The concentrations for both pMA and 2-NT are 1 mM. Laser power for SERS excitation is 3 mW and spectrometer integration time is 5 s.

■ ASSOCIATED CONTENT

Supporting Information

Additional information on the measurement setup, calculation of SERS enhancement factors, and a video showing trapping of Ag nanoparticles. This material is available free of charge via the Internet at http://pubs.acs.org.

dx.doi.org/10.1021/nl304069n | Nano Lett. XXXX, XXX, XXX–XXX

AUTHOR INFORMATION

Corresponding Author

*E-mail: kcrozier@seas.harvard.edu.

Notes

The authors declare no competing financial interest.

ACKNOWLEDGMENTS

This work was supported (in part) by the National Science Foundation (NSF) under Grant ECCS-0747560 (CAREER award) and (in part) by the Defense Advanced Research Projects Agency (DARPA) N/MEMS S&T Fundamentals program under Grant N66001-10-1-4008 issued by the Space and Naval Warfare Systems Center Pacific (SPAWAR). Fabrication work was carried out at the Harvard Center for Nanoscale Systems, which is supported by the NSF.

REFERENCES

(1) Nie, S.; Emory, S. *Science* **1997**, *275*, 1102−1106.
(2) Haynes, C. L.; McFarland, A. D.; Duyne, R. P. V. *Anal. Chem.* **2005**, *77*, 338A−346 A.
(3) Choi, I.; Choi, Y. *IEEE J. Sel. Top. Quantum Electron* **2012**, *18*, 1110−1121.
(4) Zhang, X.; Young, M.; Lyandres, O.; Van Duyne, R. P. *J. Am. Chem. Soc.* **2005**, *127*, 4484−9.
(5) Dasary, S. S. R.; Singh, A. K.; Senapati, D.; Yu, H.; Ray, P. C. *J. Am. Chem. Soc.* **2009**, *131*, 13806−12.
(6) Mulvihill, M.; Tao, A.; Benjauthrit, K.; Arnold, J.; Yang, P. *Angew. Chem.* **2008**, *120*, 6556−6560.
(7) Lin, M.; He, L.; Awika, J.; Yang, L.; Ledoux, D. R.; Li, H.; Mustapha, A. *J. Food Sci.* **2008**, *73*, T129−34.
(8) Lyandres, O.; Shah, N. C.; Yonzon, C. R.; Walsh, J. T.; Glucksberg, M. R.; Van Duyne, R. P. *Anal. Chem.* **2005**, *77*, 6134−9.
(9) Rivas, L.; Sanchez-Cortes, S.; Garcia-Ramos, J. *Langmuir* **2001**, 574−577.
(10) Leopold, N.; Lendl, B. *J. Phys. Chem. B* **2003**, *107*, 5723−5727.
(11) Mock, J. J.; Norton, S. M.; Chen, S.-Y.; Lazarides, A. A.; Smith, D. R. *Plasmonics* **2010**, *6*, 113−124.
(12) He, L.; Lin, M.; Li, H.; Kim, N.-J. *J. Raman Spectrosc.* **2009**, *41*, 739−744.
(13) Ciou, S.; Cao, Y.; Huang, H.-C.; Su, D.; Huang, C. *J. Phys. Chem. C* **2009**, *113*, 9520−9525.
(14) Diebold, E. D.; Mack, N. H.; Doorn, S. K.; Mazur, E. *Langmuir* **2009**, *25*, 1790−4.
(15) Zhu, W.; Banaee, M. G.; Wang, D.; Chu, Y.; Crozier, K. B. *Small* **2011**, *7*, 1761−6.
(16) Wang, D.; Zhu, W.; Chu, Y.; Crozier, K. B. *Adv. Mater.* **2012**, *24*, 4376−80.
(17) Banaee, M. G.; Crozier, K. B. *ACS Nano* **2011**, *5*, 307−14.
(18) Bigelow, N. W.; Vaschillo, A.; Iberi, V.; Camden, J. P.; Masiello, D. J. *ACS Nano* **2012**, *6*, 7497−504.
(19) Chu, Y.; Wang, D.; Zhu, W.; Crozier, K. B. *Opt. Express* **2011**, *19*, 14919−28.
(20) Lin, S.; Schonbrun, E.; Crozier, K. *Nano Lett.* **2010**, *10*, 2408−11.
(21) Lin, S.; Crozier, K. B. *Opt. Lett.* **2009**, *34*, 3451−3453.
(22) Cai, H.; Poon, A. W. *Opt. Lett.* **2011**, *36*, 4257−9.
(23) Mejia, C. A.; Huang, N.; Povinelli, M. L. *Opt. Lett.* **2012**, *37*, 3690.
(24) Svedberg, F.; Li, Z.; Xu, H.; Käll, M. *Nano Lett.* **2006**, *6*, 2639−41.
(25) Tong, L.; Righini, M.; Gonzalez, M. U.; Quidant, R.; Käll, M. *Lab Chip* **2009**, *9*, 193−5.
(26) Hwang, H.; Han, D.; Oh, Y.-J.; Cho, Y.-K.; Jeong, K.-H.; Park, J.-K. *Lab Chip* **2011**, *11*, 2518−25.
(27) Lin, S.; Crozier, K. B. *Opt. Express* **2012**, *20*, 3367.
(28) Lin, S.; Crozier, K. B. *Lab Chip* **2011**, *11*, 4047−51.
(29) Jackson, J. B.; Halas, N. J. *Proc. Natl. Acad. Sci. U.S.A.* **2004**, *101*, 17930−5.
(30) Ru, E. C. L.; Blackie, E.; Meyer, M.; Etchegoin, P. G. G. *J. Phys. Chem. C* **2007**, *111*, 13794−13803.